

Shining a light on NAD- and NADP-based metabolism in plants

Edward N. Smith^{*,1}, Markus Schwarzländer², R. George Ratcliffe¹, Nicholas J. Kruger¹

¹Department of Plant Sciences, University of Oxford, Oxford OX1 3RB, UK

²Institute of Plant Biology and Biotechnology (IBBP), Westfälische Wilhelms-Universität Münster, D-48143 Münster, Germany

*Correspondence: edward.smith@plants.ox.ac.uk, @tednsmith (E.N. Smith)

Keywords: NAD, NADP, biosensors, redox, pyridine nucleotides

Abstract

The pyridine nucleotides NAD(H) and NADP(H) simultaneously act as energy transducers, signalling molecules and redox couples. Recent research into photosynthetic optimisation, photorespiration, immunity, hypoxia/oxygen signalling, development, and post-harvest metabolism have all identified pyridine nucleotides as key metabolites. Further understanding in these topics requires accurate description of NAD(P)(H) metabolism, and genetically encoded fluorescent biosensors have recently become available for this purpose. Although these biosensors have begun to provide novel biological insights, their limitations must be considered and the information they provide appropriately interpreted. Here we provide a framework for understanding NAD(P)(H) metabolism and explore what fluorescent biosensors can, and cannot, tell us about plant biology, looking ahead to the pressing questions that could be answered with further development of these tools.

Pyridine nucleotides are central to plant biology

Nicotinamide adenine dinucleotide (NAD) and the phosphorylated form, nicotinamide adenine dinucleotide phosphate (NADP), are vital energy transducers and signalling molecules in all living organisms. In plants, these pyridine nucleotides serve many functions from central energy metabolism, to development and immunity (Figure 1) [1–11]. The primary role of NAD(H) is to transfer electrons from the oxidation of substrates into the mitochondrial electron transport chain, generating the proton gradient required to synthesise ATP [12]. NADPH provides a supply of reducing power for biosynthesis, oxidative stress responses and maintenance of thiol redox networks [8]. These contrasting roles are reflected in the ratios of reduced to oxidised forms, with a ratio of NADPH:NADP⁺ greater than one and a ratio of NADH:NAD⁺ less than one generally observed [13–16] (Table 1). However, the concentrations and ratios of pyridine nucleotides can vary between different

tissues and compartments, as well as depending on the conditions experienced by the plant and the quantification method used [13–19]. Redox reactions involving pyridine nucleotides also provide a link between pH and redox metabolism as the reduction of NAD(P)^+ is accompanied by release of a proton, ultimately coupling redox energy to proton gradients and ATP levels [20,21]. Beyond energy metabolism pyridine nucleotides have both intra- and extracellular signalling roles, affecting gene expression, protein modification, and cell death and survival [1–3] (Figure 1).

The involvement of NAD(P)(H) in metabolism can be described in several ways (Figure 2). Both the total concentrations of NAD(H) and NADP(H) , and the concentrations of specific reduced/oxidised forms, are important for signalling and regulation [1–3]. Each of these concentrations is made up of protein-bound and free pools, which can vary depending on the proteins present and their respective NAD(P)(H) binding affinities [15,22,23]. The redox potentials, defined by the relative concentrations of reduced/oxidised forms and influenced by local pH, are important for determining reaction directionality and the flow of reducing power. The rate of interconversion between reduced and oxidised forms (the redox flux) is important for energy metabolism and redox homeostasis [24]. Finally, synthesis and breakdown of NAD(P)(H) is important for post translational protein modification, gene expression, and cell death and survival [1–3]. These parameters are related but can vary separately from each other, and therefore accurate quantification of each of these parameters is vital for fully understanding NAD(P)(H) metabolism. Recently, genetically encoded fluorescent biosensors for pyridine nucleotides have been expressed in plants, providing measurements of NADH:NAD^+ ratios and relative measurements of free NADPH concentrations [17,18]. In this review we evaluate the application of these biosensors to plants, explore their strengths and limitations, and set out the future work needed to gain a complete understanding of NAD(P)(H) metabolism in plants.

Quantifying NAD(P)(H) concentrations and ratios

Analytical methods for quantifying pyridine nucleotides are typically destructive, relying on total cell extraction and combining of different NAD(P)(H) pools followed by enzymatic or LC-MS based analysis [25–27]. However, the concentrations of NAD(P)(H) and ratios of reduced and oxidised forms differ considerably between tissues, cells and subcellular compartments (Table 1), and therefore compartment specific information is key to

quantifying NAD(P)(H) metabolism and understanding its functional roles in plant cells [13–16,19]. Subcellular fractionation methods aim to measure compartment-specific concentrations, but artefacts can arise during extraction from exchange between compartments and interconversion of reduced and oxidised species [28]. Recently developed techniques using rapid affinity purification of organelles attempt to overcome these limitations [29], but still suffer from metabolite loss and rapid redox interconversion during extraction [30]. Non-aqueous fractionation currently provides the most reliable estimates of subcellular NAD(P)(H) concentrations by fixing metabolism prior to extraction, but methods are generally laborious, and can still give incomplete resolution of subcellular compartments [13–16,19]. Furthermore, destructive analytical methods do not distinguish between protein bound and free pools of metabolites, which can differ by several orders of magnitude [15,22]. In principle, the development of non-invasive organelle-specific measurement tools would address many of the shortcomings of the destructive analytical methods. The intrinsic autofluorescence of NAD(P)H can provide a non-invasive measure of total NAD(P)H concentration but the failure to be able to discriminate between NADH and NADPH, and inability to measure the oxidised forms of these pyridine nucleotides limit this method [22,31]. Fluorescence lifetime imaging of NAD(P)H autofluorescence can distinguish between protein-bound NADH and NADPH but is technically demanding and has not yet been established in plants [23]. In contrast, genetically encoded fluorescent biosensors offer an ideal solution allowing real-time, non-destructive, measurement of dynamic changes in specific metabolites with greater temporal and spatial separation than other methods.

Biosensors for many metabolites have been applied to plants [32], including sensors for calcium [32], potassium [33], zinc [34], chloride [35], pH [36], glucose [37], glutamate [38], ATP [39], phosphate [40], abscisic acid [41], auxin [42], gibberellin [43], hydrogen peroxide [44] and, glutathione [45] as well as thioredoxin redox potential [46]. The basic principle of metabolite sensitive fluorescent biosensors is to fuse a ligand binding domain to one or two fluorescent proteins, coupling a conformational change upon ligand binding to a change in fluorescence. Two fluorescent signals are required to allow ratiometric analysis which generates an internally normalised signal independent of the biosensor protein expression level. Absolute ligand concentrations can then be calculated by determining the binding and response properties of sensors *in vitro*, and by *in vivo* calibration (Box 1). There are some

disadvantages of this approach, including the measurement of only a single parameter at a time, the need for genetic transformation, and the risk of potential artefacts caused by pH or inaccurate calibration. However these are compensated by several important advantages including: the ability to measure real time kinetics of transient events, such as the initiation of photosynthesis; strict cell type, tissue or compartment specificity through the use of subcellular localisation tags or specific promoters; exquisite specificity for the analyte they measure; and quantification of the free pools of metabolites, mimicking the conditions experienced by endogenous enzymes. Collectively these advantages cannot be achieved with any other method.

SoNar, iNap and Peredox-mCherry are NAD(P)(H) sensors expressed in plants

Just three of the growing number of fluorescent protein-based NAD(P)(H) biosensors [47] have been expressed in plants so far: two different NADH:NAD⁺ ratio sensors, SoNar and Peredox-mCherry; and the NADPH sensors of the iNap family [17,18] (Figure 3)(Table 2). These sensors have already been used to initiate the exploration of several aspects of plant biology including: reductant flow during photosynthesis and photorespiration, immune responses, stomatal development, hypoxia, and tissue specific differences in pyridine nucleotide levels and redox poise [17,18,48–50]. However, this work has only set a starting point and there is a wide field of open questions that may be addressed by the new sensors and techniques to provide a more complete picture of pyridine nucleotide metabolism in plants.

Biosensors must have appropriate binding affinities to be used in plants

To accurately measure NAD(P)(H) concentrations in plants, biosensors must have binding affinities that match the physiology to be monitored. The binding affinity as well as the Hill coefficient set the operational range of the sensor (see Glossary). Both SoNar and Peredox-mCherry were able to detect increases in the NADH:NAD⁺ ratio suggesting they were not saturated under physiological conditions in the cytosol of *Arabidopsis* leaf and cotyledon tissues in the dark [17,18]. However, the operational range of SoNar is much greater than that of Peredox-mCherry which became saturated under certain conditions, such as supply of exogenous sucrose [17,51,52]. Therefore, a lower affinity variant, Peredox-mCherry DS, was developed by mutating the NADH binding site to increase the maximum NADH:NAD⁺ ratio that could be measured [17]. Different iNap variants were required in different

compartments to avoid saturation of the sensor in *Arabidopsis* cotyledons, with the higher affinity iNap1 being suited to the cytosol and lower affinity iNap4 being suited to plastids and peroxisomes, consistent with the higher NADPH concentration expected in these compartments [18]. Choosing a sensor with an appropriate operational range for the tissue or compartment being studied is vital for accurate quantification and online tools such as 'SensorOverlord' can assist in making this choice [53].

Biosensors can be targeted to specific subcellular compartments

Subcellular localisation tags can be added to biosensor proteins to target them to specific organelles. Peredox-mCherry has so far been localised to only the cytosol and nucleus in plants [17]; whereas SoNar has been targeted to the cytosol and plastid stroma [18]; and iNap has been targeted to the cytosol, plastid stroma and peroxisomes [18] (Table 2). Localising NAD(P)(H) biosensors to the mitochondria would be extremely useful, particularly for understanding shuttling of reducing equivalents during photosynthesis and photorespiration. However, current efforts have been unsuccessful with a lack of transformants pointing to an issue with embryo viability [17,18]. Attempts to express biosensors for other metabolites in the mitochondria have generated aberrant developmental phenotypes in several cases suggesting a common mechanism for compromised growth, rather than sequestration of a specific ligand [39]. The relatively large size of some biosensors; including SoNar, iNap and Peredox-mCherry, in combination with their irreversible maturation may not be compatible with the mitochondrial import machinery which could explain why smaller biosensors such as cpYFP localise to mitochondria without causing gross phenotypic perturbations [54]. To overcome the limitations in mitochondrial localisation, efforts should be made to design smaller biosensors, generate split designs for existing sensors [55], or to build on the recent advances in editing the plant mitochondrial genome [56].

Biosensors must be calibrated to measure absolute concentrations or redox states

Comparing measurements between different experiments or incorporating data into models requires absolute quantification of NAD(P)(H) concentrations and ratios rather than just relative changes. Sensors are typically calibrated by measuring the dissociation constant (K_d) in conditions which match those *in vivo* as closely as possible and identifying the fluorescent signal which equates to completely saturated or desaturated sensor *in vivo* (Box 1).

However, driving the *in vivo* concentration of NAD(P)(H) to the extreme values required for calibration can be challenging because of the ability of metabolism to buffer changes in metabolite concentration and the fact that NAD(P)(H) are not readily membrane permeable. To saturate the sensor, cells may be first permeabilised with digitonin and then supplied with exogenous ligand, whilst complete desaturation relies on chemical treatment to decrease the NAD(P)(H) concentration [18,52,57]. Recently, direct microinjection has been used to calibrate an inorganic phosphate biosensor in *Arabidopsis* roots [40] and a similar approach could be attempted for NAD(P)(H).

Current NAD(P)(H) sensors expressed in plants have not been used for absolute quantification, although Steinbeck et. al. (2020) used Peredox-mCherry to make an estimate of NADH:NAD⁺ ratio in the order of 0.001, assuming a cytosolic NAD⁺ concentration of 500 μ M [14,17]. This is in agreement with the ratio of free NADH:NAD⁺ estimated by equilibrium measurement with malate dehydrogenase [15]. These estimates of the free NADH:NAD⁺ ratio are an order of magnitude lower than that measured by subcellular fractionation [14] (Table 1), and suggest a substantial amount of cytosolic NADH may be bound to proteins. Using these estimates of the NADH:NAD⁺ ratio and NAD⁺ concentration, free NADH could be as low as about 0.5 μ M in the cytosol [17]. In this situation, potential competition between NADPH and NADH for binding to Peredox-mCherry deserves consideration as potential confounding factor, the reason being that a physiological NADH concentration of 0.5 μ M is close to the sensor K_d for NADH (determined at 1.2 μ M in the presence of 500 μ M NAD⁺), but also physiological NADPH concentrations of around 150 μ M are within the operational range of the sensor for NADPH (K_d determined at 531 μ M in the presence of 150 μ M NADP⁺) [17]. This rough comparison, however, is based on K_d values measured for the NAD and NADP systems in isolation of one another. Under competition with physiological concentrations of NADH and NAD⁺ for binding, NADPH is unlikely to have any impact. Direct validation would require *in vitro* calibration of the sensor protein with all four of the species (NAD⁺, NADH, NADP⁺ and NADPH) competing for binding at physiological concentrations; most importantly a determination of the K_d for NADPH in the presence of 500 μ M NAD⁺ and/or 0.5 μ M NADH. Furthermore, the side-by-side comparison between differential *in vivo* response dynamics of Peredox-mCherry and iNap, will be suited to empirically validate the specificities of both sensors *in planta*.

Lim et. al. (2020) used the high and low affinity iNap sensor variants 1 and 4 to establish that the NADPH concentration was higher in plastids than in the cytosol, consistent with results from non-aqueous fractionation [13–16,19], but did not calculate any absolute concentrations. The lack of absolute quantification is a weakness in the current application of many fluorescent biosensors particularly if the data are to be compared between independent systems or incorporated into computational models. The development of meaningful calibration protocols will be a necessary next step for the sensors to realise their full potential.

Potential effects of total pool size must be considered for NAD(P)H:NAD(P)⁺ ratio sensors

The total pool size of both reduced and oxidised pyridine nucleotides can vary between cell compartments and cell types and change dynamically under different conditions, even when the ratio of reduced to oxidised forms remains constant (Figure 2). An ideal sensor to monitor the NADH:NAD⁺ or NADPH:NADP⁺ ratio is independent of the total pool of reduced and oxidised forms. SoNar has been suggested to fulfil this criterion since binding of NADH and NAD⁺ causes changes in fluorescence signal at different positions in the spectra [52]. The response of SoNar to the NADH:NAD⁺ ratio has been shown to be independent of total NAD(H) concentration, over the range 100–400 μM [52]. By contrast, only NADH binding changes the fluorescent properties of Peredox-mCherry whereas NAD⁺ competes for the binding site but does not directly change the fluorescence. Peredox-mCherry is therefore sensitive to the total NAD(H) concentration and a ~3-fold change in NAD(H) concentration caused a ~2-fold change in the sensor midpoint for the NADH:NAD⁺ ratio, whereas in an ideal sensor the midpoint would remain the same [51]. This has implications for using Peredox-mCherry in situations where the total NAD(H) concentration may change [58]. Current interpretation of Peredox-mCherry data in plants relies on the assumption that differences in NAD⁺ or total NAD(H) concentration are minimal in relation to changes in the NADH concentration or NADH:NAD⁺ ratio [17]. This assumption is justified by the very high relative NAD⁺ levels as compared to NADH (potentially up to 1000-fold [15]), meaning that a large fold-change in NADH concentration will result in only a minor fractional-change in NAD⁺ concentration [17]. However, there are plausible exceptions. Application of Peredox-mCherry to study stomatal development in *Arabidopsis* found external application of NAD⁺ increased the apparent cytosolic NADH:NAD⁺ ratio whilst total cellular NAD⁺ concentration

also increased [49]. The increase in sensor ratio may either reflect an increase in NADH:NAD⁺ or alternatively be caused by an increased total NAD(H) pool. In such a situation when both NADH:NAD⁺ and major NAD(H) concentration changes may be expected, the system is not sufficiently described by Peredox-mCherry and therefore SoNar or an NAD⁺ specific sensor may be required for clarification.

pH sensitivity of fluorescent biosensors for NAD(P)(H)

pH differs between compartments and cell types and can change dynamically and markedly (up to 1.5 pH units) during fluctuations in photosynthesis, hypoxia or calcium signalling [18,50,59]. Fluorescent proteins can be intrinsically pH sensitive and several of the fluorescent protein variants used in biosensors are particularly susceptible since the chromophore is exposed to the medium as a result of the circular permutation [54,60,61]. Therefore, when measuring NAD(P)(H), any confounding effect of pH on biosensor readout must be considered. Peredox-mCherry has the advantage of being largely unaffected by pH over a physiologically relevant range, relying on a pH-insensitive variant of the cpT-Sapphire fluorescent protein and an additional mutagenesis of the Rex domains to produce the final pH-insensitive sensor [17,51]. By contrast, iNap and SoNar are strongly affected by pH when excited at 485 nm whereas excitation at 420 nm is relatively insensitive to pH [18,52,62]. To overcome this pH sensitivity, an NAD(P)(H)-insensitive control sensor with a similar pH response, iNapC, is expressed in separate transgenic plants under the same conditions to correct for changes in pH. The need for a separate plant to correct for pH effects can complicate experiments using iNap and SoNar and makes tissue/cell specific visualisation of NAD(P)(H) levels more challenging. Peredox-mCherry therefore has a major advantage, particularly when creating cell-specific maps or examining processes associated with pH changes [17,48]. An iNap-mCherry construct has been created to avoid use of the pH sensitive fluorescence signal when quantifying NADPH levels, but this sensor shows a lower dynamic range and is yet to be tested in plants [62].

Fluorescence lifetime imaging can help to avoid pH sensitivity

Current applications of fluorescent sensors for NAD(P)(H) in plants have relied on fluorescent intensity measurement to quantify metabolite concentrations. However, fluorescence lifetime imaging (FLIM) can be used as an orthogonal readout to quantify sensor responses with strengths and limitations that complement those of fluorescence

intensity measurements. Typically FLIM relies on measuring the time between excitation and emission of fluorescence rather than the overall intensity [63]. A further feature of FLIM applied to fluorescent biosensors is based on the deconvolution of fluorescence decay into multiple components [64–66]. The ratio of these decay components can produce a robust signal that is independent of sensor concentration and relies on only a single fluorescence excitation/emission wavelength. Therefore, time resolved fluorescence allows the single pH-independent fluorescent signal upon excitation at 420 nm of iNap and SoNar to be used, eliminating the need for correction with separate transgenic plants expressing iNapC [64–66]. The dynamic range of time resolved fluorescence measurements can also be greater than intensity-based measurements which can potentially improve signal-to-noise ratios. For example, the dynamic range of Peredox increased from 3-fold to 7-fold when time resolved fluorescence was used [64]. Since FLIM is independent of sensor abundance, fusion of Peredox to mCherry is no longer necessary, reducing the size of the protein with potential advantages for expression and subcellular targeting (see section on ‘Biosensors can be targeted to specific subcellular compartments’) [17]. Engineering new sensors focusing on fluorescence lifetime properties rather than fluorescence intensities might open new possibilities for sensor designs that have previously been overlooked [65].

An NAD⁺ specific sensor is needed for plants

Changes in the NADH:NAD⁺ ratio can be caused by differences in the rate of oxidation and reduction of NAD(H) and also by direct synthesis or breakdown of NADH or NAD⁺ (Figure 2). Measuring the NADH:NAD⁺ ratio alone cannot distinguish between these possibilities and therefore separate measurements of NADH, NAD⁺, or the total pool of NAD(H) are required. For example, Peredox-mCherry measured an increase in the NADH:NAD⁺ ratio upon flg22 pathogen elicitor treatment [17]. However, by measuring the NADH:NAD⁺ ratio alone it is not clear to what extent this was driven by breakdown of NAD⁺, *de novo* synthesis of NADH, or reduction of NAD⁺ to generate NADH. Peredox-mCherry DS, the lower affinity variant of Peredox-mCherry, acts more like an NADH sensor, independent of the NAD⁺ concentration. Peredox-mCherry DS also showed an increase in response to flg22 treatment suggesting the increased NADH:NAD⁺ ratio is driven at least partly by an increase in NADH concentration rather than just degradation of NAD⁺ [17]. Alternative sensors are available that have yet to be expressed in plants including Frex, an NADH sensor, and LigA-cpVenus, an NAD⁺ specific

sensor (Table 2) [67,68]. However, these sensors have limitations for application to plants. Frex is highly pH sensitive, similar to other cpYFP based sensors SoNar and iNap [67]. Unfortunately FLIM of Frex relies on the pH-sensitive excitation at 485 nm and therefore pH correction would still be required to use this sensor in plants [64,65]. Similarly the NAD⁺ sensor LigA-cpVenus is pH-sensitive and would require separate transgenic plants expressing cpVenus for pH correction akin to SoNar and iNap [68]. Moreover the *in vitro* K_d of Frex and LigA-cpVenus suggest these sensors could be saturated in plants. However, ultimately, their suitability for quantifying changes in NAD(H) concentration will need to be tested empirically since *in vitro* and *in vivo* binding affinities can differ [68].

An NADPH:NADP⁺ and/or an NADP⁺ sensor are needed for plants

Whilst NADPH sensing using iNap has been used to draw conclusions on reductant flow between compartments from photosynthesis and photorespiration [18], the actual redox potentials of the subcellular NADP(H) pools are dependent on the ratios of reduced to oxidised forms. Therefore, a more meaningful definition of the system could be achieved with an NADPH:NADP⁺ ratio sensor, which has not yet been developed, or an NADP⁺ specific sensor in combination with the current iNap NADPH sensor in plants. Two NADP⁺ sensors have been developed and used in bacteria and mammalian cells, Apollo-NADP⁺ and NADPsor, although both suffer from small dynamic ranges and the binding affinity of NADPsor is likely too weak to be useful *in planta* (Table 2) [69,70]. Therefore, these existing NADP⁺ biosensors would require modification before they can be applied to plants.

As well as extending the use of existing biosensors to plants, completely new sensors also need to be developed (Table 2). An NADPH:NADP⁺ ratio sensor to directly report on the NADPH redox potential would be useful and could be constructed as a ligand binding sensor, similar to SoNar or Peredox. Alternatively, consideration should be given to a thiol-based redox sensor, which is directly oxidised or reduced by NADP(H). One such sensor could be created by fusing an NADP-specific glutathione reductase to a roGFP, analogous to the glutathione redox sensors that are based on fusion of glutaredoxin and roGFP [71]. Since NAD-specific glutathione reductase isoforms have also been described [72] the same sensor design with a different glutathione reductase domain could allow sensing of the NAD(H) redox potential.

Concentration alone is not enough to describe NAD(P)(H) metabolism

Fluorescent biosensors report on concentrations or ratios of metabolites and do not directly inform about the underlying metabolic fluxes. Fluxes can vary independently of concentrations [73,74] and a flux may change without any detectable change in the steady state concentration of NAD(P)(H). An example where the steady state readout of biosensors can be open to multiple interpretations is understanding the hypoxic niche of plant meristems. Plant meristems exist in low oxygen environments which are important for their function, but it remains unclear how tissues maintain this state and what the relative roles of metabolism and physical separation are in achieving low oxygen concentrations [75,76]. A low NADH:NAD⁺ ratio was identified in the shoot apical meristem (SAM) region using Peredox-mCherry [17]. This contrasts with the high NADH:NAD⁺ observed in other plant tissues under low external oxygen conditions [17,50] and could be the result of the high respiratory flux required to consume oxygen and maintain a hypoxic environment. However, low ATP concentrations have also been identified in the SAM region [39], which would typically be associated with inhibition of respiration. Measurements of the concentrations of these metabolites in isolation are uninformative, as the steady state concentrations of ATP, oxygen, and NAD(H) do not necessarily reflect their rates of consumption. Combining Peredox-mCherry or SoNar and new oxygen biosensors [77] with specific genetic knockouts could still help identify the genes responsible for maintaining the low oxygen environment in the SAM, but the currently available sensors alone do not reveal the metabolic fluxes associated with the low oxygen state.

Dynamic changes in metabolite concentration can be more informative than steady state levels as a change in concentration over time must be caused by a difference between the rates of production and consumption of a metabolite. Increased flux into reductant production when leaves are illuminated causes an increase in the NADH:NAD⁺ ratio in the cytosol due to export of reducing equivalents from the chloroplast [17,18,48]. To identify the mechanism leading to the increased cytosolic NADH:NAD⁺ ratio, Elsässer et al. (2020) abolished expression of genes encoding isozymes of malate dehydrogenase (MDH) specific to different compartments [48]. However, the dynamics of the cytosolic NADH:NAD⁺ increase upon illumination remained similar, suggesting compensatory fluxes can maintain reductant export. However, using fluorescent biosensors alone it is not possible to

determine which fluxes have changed to maintain reductant export in the MDH knock out plants. Thus, whilst measurement of dynamic changes using fluorescent biosensors can provide some information about changes in flux, direct measurement of the fluxes associated with NAD(P)(H) metabolism are needed for a complete understanding.

Isotopic labelling can quantify redox fluxes and rates of synthesis/breakdown

Directly measuring the underlying fluxes that support NAD(P)(H) metabolism provides a mechanistic basis to explain plant biology, whereas fluorescent biosensors only report on the effects of these changes in flux. Typical flux analysis methods in plants are based on tracing isotopically labelled carbon (^{13}C) through metabolic networks. However, redox reactions involving pyridine nucleotides transfer hydrogen and electrons rather than carbon atoms and therefore isotopically labelled carbon cannot be used to directly quantify redox fluxes. This problem is exacerbated for reactions such as isocitrate dehydrogenase which, depending on the isoform, can produce either NADH or NADPH via an identical carbon transformation [14]. Using isotopically labelled hydrogen (deuterium, ^2H) rather than carbon can overcome this limitation by specifically quantifying fluxes through redox reactions, as has been demonstrated in mammalian cells [78–82]. However, the application of deuterium labelling strategies in plants is limited by the structure of the plant metabolic network and the effect of hydrogen-deuterium exchange with water [83]. Overcoming this in plants remains a challenge, but with different labelling strategies or in different plant tissues, deuterium labelling may be able to quantify fluxes through NAD(P)(H) redox reactions. NAD(P)(H) redox fluxes can still be indirectly estimated using ^{13}C flux analysis, but this relies on assumptions about relative contributions of different isozymes and their coenzyme specificity, which are difficult to validate *in vivo* [84–87].

Beyond redox interconversion the direct synthesis and breakdown of NAD(P)(H) is important for photosynthesis, calcium signalling, immunity, development and gene expression [1,2,6,7,10]. NAD^+ is synthesised *de novo* from aspartate or salvaged from various intermediates [7] while NADP^+ is generated by phosphorylation of NAD^+ by NAD-kinases [88] (Figure 2). NAD(P)(H) can be directly catabolised by adenosine diphosphate ribose cyclase, NAD-glycohydrolase, poly-ADPribose polymerases, sirtuins and NUDIX hydrolase [1,7] (Figure 2). The pathways of biosynthesis and recycling of pyridine nucleotides in plants were originally identified using radiolabelling [89–92] and future studies could combine ^{13}C -

labelling and LC-MS to measure changes in rates of synthesis/breakdown of NAD(P)(H) under different conditions [93,94]. Quantifying how the metabolic network meets the demands of NAD(P)(H) catabolising enzymes could help explain the coordination of metabolic activity with gene expression.

Integrating concentration measurements into computational models improves definition of metabolic networks

Integrating measurements of compartment specific concentrations and ratios from fluorescent biosensors can improve the accuracy of computational models. Such models could be kinetic, based on dynamic concentration information and enzyme parameters [95,96], or stoichiometric, based on flux balance analysis (FBA) with additional thermodynamic constraints to incorporate metabolite concentrations [97]. A kinetic model of mammalian mitochondrial redox metabolism incorporating data from a mitochondrially targeted iNap3 sensor and ^{13}C -flux analysis has recently been used to investigate mitochondrial NADPH production rate and NADPH:NADP⁺ ratios under H₂O₂ redox stress [57]. By measuring biosensor dynamics at various rates of H₂O₂ production, data were fitted to a kinetic model [57]. Methods using whole cell extracts are unable to provide the required data for kinetic modelling, demonstrating the advantage of *in vivo* biosensors. A similar approach could be taken to study dynamic changes in plant metabolism currently inaccessible to steady state flux analysis, such as during pathogen infection.

Parameters for thermodynamically constrained FBA models could also be provided by *in vivo* measurement of NAD(P)(H) concentrations or redox states using fluorescent biosensors helping, for example, to resolve the directionality of metabolite shuttles between organelles [97,98]. The direction of readily reversible reactions such as the malate-oxaloacetate shuttle is heavily influenced by the relative concentrations of NAD(H) in different compartments. Therefore, quantitative measurement of subcellular NADH:NAD⁺ ratios in the cytosol and mitochondria using fluorescent biosensors would provide the necessary information to quantify the direction of reductant flow between compartments. SoNar and iNap have already been used to measure the comparative differences in the amount of redox coenzymes in different compartments, supporting hypotheses of reductant flow during photosynthesis and photorespiration [18]. However, sensor calibration and quantification of

absolute concentrations or ratios is required for incorporation into models for flux prediction.

Concluding remarks and future perspectives

Fluorescent sensors for the NADH:NAD⁺ ratio and NADPH concentration have already provided insight into plant immunity, development and energy metabolism [17,18,48,49]. Application of new sensors for the NAD(P)⁺ concentration and NADPH:NADP⁺ ratio are required to generate a complete picture of both the redox and signalling roles of pyridine nucleotides (Table 2). Fluorescent biosensors cannot quantify the underlying redox and synthesis/breakdown fluxes of NAD(P)(H), but the compartment specific data they generate can provide useful constraints for computational models. Accurate calibration is vital for providing quantitative data but remains a challenge for NAD(P)(H) sensors. Future work using both existing and novel sensors should take advantage of time resolved fluorescence methods to avoid pH sensitivity and improve dynamic range. Further refinement of current approaches, expression of new sensors in plants and integration of the ensuing information into flux models will all be needed to help develop a better understanding of NAD(P)(H) metabolism in the future. Fluorescent biosensors have begun to shine a light on pyridine nucleotide-based metabolism in plants, and offer the potential to illuminate a range of biological problems in the future (see Outstanding Questions).

Acknowledgments: This work was supported by funding from the Biotechnology and Biological Sciences Research Council (BBSRC) [BB/M011224/1]. Figures were created with BioRender.com

References

- 1 Gakière, B. *et al.* (2018) More to NAD⁺ than meets the eye: a regulator of metabolic pools and gene expression in Arabidopsis. *Free Radic. Biol. Med.* 122, 86–95
- 2 Hashida, S.N. *et al.* (2009) The role of NAD biosynthesis in plant development and stress responses. *Ann. Bot.* 103, 819–824
- 3 Hunt, L. *et al.* (2004) NAD - New roles in signalling and gene regulation in plants. *New Phytol.* 163, 31–44
- 4 Aghdam, M.S. *et al.* (2020) NADPH as a quality footprinting in horticultural crops

- marketability. *Trends Food Sci. Technol.* 103, 152–161
- 5 Pétriacq, P. *et al.* (2013) NAD: Not just a pawn on the board of plant-pathogen interactions. *Plant Signal. Behav.* 8, e22477
 - 6 Pétriacq, P. *et al.* (2016) Pyridine nucleotides induce changes in cytosolic pools of calcium in Arabidopsis. *Plant Signal. Behav.* 11, 1–3
 - 7 Gakière, B. *et al.* (2018) NAD⁺ biosynthesis and signaling in plants. *Crit. Rev. Plant Sci.* 37, 259–307
 - 8 Foyer, C.H. and Noctor, G. (2009) Redox regulation in photosynthetic organisms: signaling, acclimation, and practical implications. *Antioxid. Redox Signal.* 11, 861–905
 - 9 Wang, C. *et al.* (2019) Extracellular pyridine nucleotides trigger plant systemic immunity through a lectin receptor kinase/BAK1 complex. *Nat. Commun.* 10, 4810
 - 10 Hashida, S. and Kawai-Yamada, M. (2019) Inter-organelle NAD metabolism underpinning light responsive NADP dynamics in plants. *Front. Plant Sci.* 10, 960
 - 11 Decros, G. *et al.* (2019) Regulation of pyridine nucleotide metabolism during tomato fruit development through transcript and protein profiling. *Front. Plant Sci.* 10, 1201
 - 12 Schertl, P. and Braun, H.P. (2014) Respiratory electron transfer pathways in plant mitochondria. *Front. Plant Sci.* 5, 163
 - 13 Szal, B. *et al.* (2008) Changes in energy status of leaf cells as a consequence of mitochondrial genome rearrangement. *Planta* 227, 697–706
 - 14 Igamberdiev, A.U. and Gardeström, P. (2003) Regulation of NAD- and NADP-dependent isocitrate dehydrogenases by reduction levels of pyridine nucleotides in mitochondria and cytosol of pea leaves. *Biochim. Biophys. Acta - Bioenerg.* 1606, 117–125
 - 15 Heineke, D. *et al.* (1991) Redox transfer across the inner chloroplast envelope membrane. *Plant Physiol.* 95, 1131–1137
 - 16 Wigge, B. *et al.* (1993) The redox levels and subcellular distribution of pyridine nucleotides in illuminated barley leaf protoplasts studied by rapid fractionation.

- 17 Steinbeck, J. *et al.* (2020) In vivo NADH/NAD⁺ biosensing reveals the dynamics of cytosolic redox metabolism in plants. *Plant Cell* 32, 3324–3345
- 18 Lim, S. *et al.* (2020) In planta study of photosynthesis and photorespiration using NADPH and NADH/NAD⁺ fluorescent protein sensors. *Nat. Commun.* 11, 3238
- 19 Herber, U.W. and Santarius, K.A. (1965) Compartmentation and reduction of pyridine nucleotides in relation to photosynthesis. *Biochim. Biophys. Acta* 9, 390–408
- 20 Igamberdiev, A.U. and Kleczkowski, L.A. (2019) Thermodynamic buffering, stable non-equilibrium and establishment of the computable structure of plant metabolism. *Prog. Biophys. Mol. Biol.* 146, 23–36
- 21 Sakano, K. (2001) Metabolic regulation of pH in plant cells: Role of cytoplasmic pH in defense reaction and secondary metabolism. *Int. Rev. Cytol.* 206, 1–44
- 22 Kasimova, M.R. *et al.* (2006) The free NADH concentration is kept constant in plant mitochondria under different metabolic conditions. *Plant Cell* 18, 688–698
- 23 Blacker, T.S. *et al.* (2014) Separating NADH and NADPH fluorescence in live cells and tissues using FLIM. *Nat. Commun.* 5, 3936
- 24 Corpas, F.J. and Barroso, J.B. (2014) NADPH-generating dehydrogenases: their role in the mechanism of protection against nitro-oxidative stress induced by adverse environmental conditions. *Front. Environ. Sci.* 2, 55
- 25 Lu, W. *et al.* (2018) Extraction and quantitation of NAD(P)(H). *Antioxid. Redox Signal.* 28, 167–179
- 26 Zhang, Y. *et al.* (2020) Adenine nucleotide and nicotinamide adenine dinucleotide measurements in plants. *Curr. Protoc. plant Biol.* 5, e20115
- 27 Queval, G. and Noctor, G. (2007) A plate reader method for the measurement of NAD, NADP, glutathione, and ascorbate in tissue extracts: Application to redox profiling during Arabidopsis rosette development. *Anal. Biochem.* 363, 58–69
- 28 Dietz, K.J. (2017) Subcellular metabolomics: The choice of method depends on the

- aim of the study. *J. Exp. Bot.* 68, 5695–5698
- 29 Luo, L. *et al.* (2020) Rapid and specific isolation of intact mitochondria from *Arabidopsis* leaves. *J. Genet. Genomics* 47, 65–68
- 30 Niehaus, M. *et al.* (2020) Rapid affinity purification of tagged plant mitochondria (Mito-AP) for metabolome and proteome analyses. *Plant Physiol.* 182, 1194–1210
- 31 Schaefer, P.M. *et al.* (2019) NADH Autofluorescence—A Marker on its Way to Boost Bioenergetic Research. *Cytom. Part A* 95, 34–46
- 32 Walia, A. *et al.* (2018) Genetically encoded biosensors in plants: pathways to discovery. *Annu. Rev. Plant Biol.* 69, 497–524
- 33 Wang, F.-L. *et al.* (2020) A mechanism for sensing of and adaptation to K⁺ deprivation in plants. *bioRxiv* DOI: 10.1101/2020.03.21.000570
- 34 Lanquar, V. *et al.* (2014) Dynamic imaging of cytosolic zinc in *Arabidopsis* roots combining FRET sensors and RootChip technology. *New Phytol.* 202, 198–208
- 35 Lorenzen, I. *et al.* (2004) Salt stress-induced chloride flux: A study using transgenic *Arabidopsis* expressing a fluorescent anion probe. *Plant J.* 38, 539–544
- 36 Gjetting, K.S.K. *et al.* (2012) Live imaging of intra-and extracellular pH in plants using pHusion, a novel genetically encoded biosensor. *J. Exp. Bot.* 63, 3207–3218
- 37 Chaudhuri, B. *et al.* (2008) Protonophore- and pH-insensitive glucose and sucrose accumulation detected by FRET nanosensors in *Arabidopsis* root tips. *Plant J.* 56, 948–962
- 38 Toyota, M. *et al.* (2018) Glutamate triggers long-distance, calcium-based plant defense signaling. *Science* 361, 1112–1115
- 39 De Col, V. *et al.* (2017) ATP sensing in living plant cells reveals tissue gradients and stress dynamics of energy physiology. *Elife* 6, e26770
- 40 Sahu, A. *et al.* (2020) Spatial profiles of phosphate in roots indicate developmental control of uptake, recycling, and sequestration. *Plant Physiol.* 184, 2064–2077
- 41 Waadt, R. *et al.* (2020) Dual-reporting transcriptionally linked genetically encoded

- fluorescent indicators resolve the spatiotemporal coordination of cytosolic abscisic acid and second messenger dynamics in arabidopsis. *Plant Cell* 32, 2582–2601
- 42 Herud-Sikimic, O. *et al.* (2020) Design of a biosensor for direct visualisation of auxin. *bioRxiv* DOI: 10.1101/2020.01.19.911735
- 43 Rizza, A. *et al.* (2017) In vivo gibberellin gradients visualized in rapidly elongating tissues. *Nat. Plants* 3, 803–813
- 44 Costa, A. *et al.* (2010) H₂O₂ in plant peroxisomes: An *in vivo* analysis uncovers a Ca²⁺-dependent scavenging system. *Plant J.* 62, 760–772
- 45 Schwarzländer, M. *et al.* (2008) Confocal imaging of glutathione redox potential in living plant cells. *J. Microsc.* 231, 299–316
- 46 Sugiura, K. *et al.* (2019) The thioredoxin (Trx) redox state sensor protein can visualize Trx activities in the light/dark response in chloroplasts. *J. Biol. Chem.* 294, 12091–12098
- 47 Zhao, Y. *et al.* (2017) Visualization of nicotine adenine dinucleotide redox homeostasis with genetically encoded fluorescent sensors. *Antioxid. Redox Signal.* 28, 213–229
- 48 Elsässer, M. *et al.* (2020) Photosynthetic activity triggers pH and NAD redox signatures across different plant cell compartments. *bioRxiv* DOI: 10.1101/2020.10.31.363051
- 49 Feitosa-Araujo, E. *et al.* (2020) Changes in intracellular NAD status affect stomatal development in an abscisic acid-dependent manner. *Plant J.* 104, 1149–1168
- 50 Wagner, S. *et al.* (2019) Multiparametric real-time sensing of cytosolic physiology links hypoxia responses to mitochondrial electron transport. *New Phytol.* 244, 1668–1684
- 51 Hung, Y.P. *et al.* (2011) Imaging cytosolic NADH-NAD⁺ redox state with a genetically encoded fluorescent biosensor. *Cell Metab.* 1071, 83–95
- 52 Zhao, Y. *et al.* (2015) SoNar, a highly responsive NAD⁺/NADH sensor, allows high-throughput metabolic screening of anti-tumor agents. *Cell Metab.* 21, 777–789

- 53 Stanley, J.A. *et al.* (2020) The SensorOverlord predicts the accuracy of measurements with ratiometric biosensors. *Sci. Rep.* 10, 16843
- 54 Schwarzländer, M. *et al.* (2011) The circularly permuted yellow fluorescent protein cpYFP that has been used as a superoxide probe is highly responsive to pH but not superoxide in mitochondria: Implications for the existence of superoxide “flashes.” *Biochem. J.* 437, 381–387
- 55 Thiel, I. V. *et al.* (2014) An atypical naturally split intein engineered for highly efficient protein labeling. *Angew. Chemie - Int. Ed.* 53, 1306–1310
- 56 Arimura, S. ichi *et al.* (2020) Targeted gene disruption of ATP synthases 6-1 and 6-2 in the mitochondrial genome of *Arabidopsis thaliana* by mitoTALENs. *Plant J.* 104, 1459–1471
- 57 Moon, S.J. *et al.* (2020) Oxidative pentose phosphate pathway and glucose anaplerosis support maintenance of mitochondrial NADPH pool under mitochondrial oxidative stress. *Bioeng. Transl. Med.* 5, e10184
- 58 Zhao, Y. *et al.* (2016) *In vivo* monitoring of cellular energy metabolism using SoNar, a highly responsive sensor for NAD⁺/NADH redox state. *Nat. Protoc.* 11, 1345–1359
- 59 Behera, S. *et al.* (2018) Cellular Ca²⁺ signals generate defined pH signatures in plants. *Plant Cell* 30, 2704–2719
- 60 Quatresous, E. *et al.* (2012) Mitochondria-targeted cpYFP: PH or superoxide sensor? *J. Gen. Physiol.* 140, 567–570
- 61 Schwarzländer, M. *et al.* (2014) The “mitoflash” probe cpYFP does not respond to superoxide. *Nature* 514, E12–E14
- 62 Tao, R. *et al.* (2017) Genetically encoded fluorescent sensors reveal dynamic regulation of NADPH metabolism. *Nat. Methods* 14, 720–728
- 63 Datta, R. *et al.* (2020) Fluorescence lifetime imaging microscopy: fundamentals and advances in instrumentation, analysis, and applications. *J. Biomed. Opt.* 25, 071203
- 64 Chang, M. *et al.* (2017) Using fractional intensities of time-resolved fluorescence to sensitively quantify NADH/NAD⁺ with genetically encoded fluorescent biosensors. *Sci.*

- 65 Li, L. *et al.* (2020) Sensitive detection via the time-resolved fluorescence of circularly permuted yellow fluorescent protein biosensors. *Sensors Actuators, B Chem.* 321, 128614
- 66 Li, L. *et al.* (2019) pH resistant ratiometric measurement of nicotinamide adenine dinucleotide levels by time-resolved fluorescence spectroscopy. *Chinese J. Anal. Chem.* 47, e19009–e19013
- 67 Zhao, Y. *et al.* (2011) Genetically encoded fluorescent sensors for intracellular NADH detection. *Cell Metab.* 14, 555–566
- 68 Cambronne, X.A. *et al.* (2016) Biosensor reveals multiple sources for mitochondrial NAD⁺. *Science* 352, 1474–1477
- 69 Cameron, W.D. *et al.* (2016) Apollo-NADP⁺: A spectrally tunable family of genetically encoded sensors for NADP⁺. *Nat. Methods* 13, 352–358
- 70 Zhao, F.L. *et al.* (2016) A genetically encoded biosensor for in vitro and in vivo detection of NADP⁺. *Biosens. Bioelectron.* 77, 901–906
- 71 Schwarzländer, M. *et al.* (2016) Dissecting redox biology using fluorescent protein sensors. *Antioxid. Redox Signal.* 24, 680–712
- 72 Reiter, J. *et al.* (2014) A novel natural NADH and NADPH dependent glutathione reductase as tool in biotechnological applications. *JSM Biotechnol. Biomed. Eng.* 2, 1028
- 73 Kruger, N.J. and Ratcliffe, R.G. (2009) Insights into plant metabolic networks from steady-state metabolic flux analysis. *Biochimie* 91, 697–702
- 74 Fell, D.A. (2005) Enzymes, metabolites and fluxes. *J. Exp. Bot.* 56, 267–272
- 75 Weits, D.A. *et al.* (2019) An apical hypoxic niche sets the pace of shoot meristem activity. *Nature* 569, 714–717
- 76 Weits, D.A. *et al.* (2020) Molecular oxygen as a signaling component in plant development. *New Phytol.* 229, 24–35

- 77 Panicucci, G. *et al.* (2020) An improved HRPE-based transcriptional output reporter to detect hypoxia and anoxia in plant tissue. *Biosensors* 10, 197
- 78 Zhang, Z. *et al.* (2017) Chemical basis for deuterium labeling of fat and NADPH. *J. Am. Chem. Soc.* 139, 14368–14371
- 79 Fan, J. *et al.* (2014) Quantitative flux analysis reveals folate-dependent NADPH production. *Nature* 510, 298–302
- 80 Lewis, C.A. *et al.* (2014) Tracing compartmentalized NADPH metabolism in the cytosol and mitochondria of mammalian cells. *Mol. Cell* 55, 253–263
- 81 Chen, L. *et al.* (2019) NADPH production by the oxidative pentose-phosphate pathway supports folate metabolism. *Nat. Metab.* 1, 404–415
- 82 Liu, L. *et al.* (2016) Malic enzyme tracers reveal hypoxia-induced switch in adipocyte NADPH pathway usage. *Nat. Chem. Biol.* 12, 345–352
- 83 Smith, E.N. *et al.* (2019) Limitations of deuterium-labelled substrates for quantifying NADPH metabolism in heterotrophic arabidopsis cell cultures. *Metabolites* 9, 205
- 84 Masakapalli, S.K. *et al.* (2010) Subcellular flux analysis of central metabolism in a heterotrophic Arabidopsis cell suspension using steady-state stable isotope labeling. *Plant Physiol.* 152, 602–619
- 85 Masakapalli, S.K. *et al.* (2013) The metabolic flux phenotype of heterotrophic Arabidopsis cells reveals a complex response to changes in nitrogen supply. *Plant J.* 74, 569–582
- 86 Masakapalli, S.K. *et al.* (2014) The metabolic flux phenotype of heterotrophic Arabidopsis cells reveals a flexible balance between the cytosolic and plastidic contributions to carbohydrate oxidation in response to phosphate limitation. *Plant J.* 78, 964–977
- 87 Suarez-Mendez, C.A. *et al.* (2016) Interaction of storage carbohydrates and other cyclic fluxes with central metabolism: a quantitative approach by non-stationary ¹³C metabolic flux analysis. *Metab. Eng. Commun.* 3, 52–63
- 88 Li, B.-B. *et al.* (2018) NAD kinases: metabolic targets controlling redox co-enzymes

- and reducing power partitioning in plant stress and development. *Front. Plant Sci.* 9, 379
- 89 Ashihara, H. *et al.* (2005) *De novo* and salvage biosynthetic pathways of pyridine nucleotides and nicotinic acid conjugates in cultured plant cells. *Plant Sci.* 169, 107–114
 - 90 Ashihara, H. *et al.* (2010) Pyridine salvage and nicotinic acid conjugate synthesis in leaves of mangrove species. *Phytochemistry* 71, 47–53
 - 91 Ashihara, H. and Deng, W.W. (2012) Pyridine metabolism in tea plants: salvage, conjugate formation and catabolism. *J. Plant Res.* 125, 781–791
 - 92 Katahira, R. and Ashihara, H. (2009) Profiles of the biosynthesis and metabolism of pyridine nucleotides in potatoes (*Solanum tuberosum* L.). *Planta* 231, 35–45
 - 93 Liu, L. *et al.* (2018) Quantitative analysis of NAD synthesis-breakdown fluxes. *Cell Metab.* 27, 1067–1080
 - 94 Bustamante, S. *et al.* (2018) Quantifying the cellular NAD⁺ metabolome using a tandem liquid chromatography mass spectrometry approach. *Metabolomics* 14, 15
 - 95 Nägele, T. *et al.* (2010) Mathematical modeling of the central carbohydrate metabolism in arabidopsis reveals a substantial regulatory influence of vacuolar invertase on whole plant carbon metabolism. *Plant Physiol.* 153, 260–272
 - 96 Baghalian, K. *et al.* (2014) Plant metabolic modeling: achieving new insight into metabolism and metabolic engineering. *Plant Cell* 26, 3847–3866
 - 97 Hamilton, J.J. *et al.* (2013) Quantitative assessment of thermodynamic constraints on the solution space of genome-scale metabolic models. *Biophys. J.* 105, 512–522
 - 98 Shameer, S. *et al.* (2019) Leaf energy balance requires mitochondrial respiration and export of chloroplast NADPH in the light. *Plant Physiol.* 180, 1947–1961
 - 99 Gloaguen, P. *et al.* (2017) ChloroKB: A web application for the integration of knowledge related to chloroplast metabolic network. *Plant Physiol.* 174, 922–934

Figures

Figure 1. Pyridine nucleotides are involved in many aspects of plant biology including, but not limited to: development [2], energy metabolism [10], signalling [6,9], ROS/RNS metabolism [8], post-harvest metabolism [4,11], gene expression [3], immunity [5] and biosynthesis. SAM – shoot apical meristem, LecRK – lectin receptor kinase, TIR – Toll/interleukin-1 receptor, RBOH – respiratory burst oxidase homologue, oxPPP – oxidative pentose phosphate pathway, ROS – reactive oxygen species, RNS – reactive nitrogen species.

Figure 2. The different parameters associated with the redox couples NADP(H) and NAD(H) at a metabolic steady state include: the concentration of NAD(P)⁺ or NAD(P)H, the rate of interconversion between reduced and oxidised forms or the redox flux, and the synthesis/breakdown flux. The steady state redox and synthesis/breakdown fluxes can vary separately from the concentrations of NAD(P)(H) and the total pool sizes of NAD(P)(H) can vary separately from the NAD(P)H:NAD(P)⁺ ratios. It is likely that changes in one parameter will be associated with changes in other parameters, particularly during the transition between metabolic steady states. However, fluxes, total concentrations, and ratios can vary separately and should be measured independently to gain a full understanding of NAD(P)(H) metabolism. ADPR – adenosine diphosphate ribose, PARP – poly-ADP-ribose polymerase, NADP⁺-Pase – NADP⁺-phosphatase, NADK – NAD-kinase, NADHK – NADH-kinase.

Figure 3. The structure and binding properties of SoNar, Peredox-mCherry and iNap. **(A)** SoNar is a dimer made from monomers containing a cpYFP (circularly permuted yellow fluorescent protein) and a Rex domain. The dimer is able to bind both NAD⁺ and NADH [52]. Binding of NADH causes an increase in cpYFP fluorescence intensity at excitation (Ex) 420 nm/ emission (Em) 520 nm whilst binding of NAD⁺ causes an increase in fluorescence intensity at Ex 485 nm/ Em 520 nm. **(B)** Peredox-mCherry is made from a cpTS (circularly permuted T-Sapphire) and two Rex binding domains fused to an mCherry fluorescent protein at the C-terminus [51]. Binding of NADH causes an increase in fluorescence intensity at Ex 400 nm/ Em 510 nm of cpTS whilst NAD⁺ competes for binding but has no direct effect on fluorescence. mCherry fluorescence at Ex 587 nm/ Em 610 nm is insensitive to NAD(H) concentration and provides an internal normalisation. **(C)** iNap is a modified form of SoNar, also made from a cpYFP and Rex domain but mutated to change the binding specificity to

bind NADPH only [62]. Binding of NADPH causes an increase in fluorescence intensity at Ex 420 nm/ Em 520 nm and a decrease in fluorescence intensity at Ex 485 nm/ Em 520 nm.

Tables

Table 1. Concentrations and ratios of NAD(P)(H) in subcellular compartments. Values are based on subcellular fractionation and analytical measurement and therefore represent total pools i.e. the sum of protein bound and free pools. Free pools of pyridine nucleotides, which biosensors are sensitive to, are likely to be lower than the values reported here [15,17,22]. Values are collated from ChloroKB [99]. See references within table for description of conditions and plant species.

Metabolite	Metabolite concentration (μM or ratio)	
	Minimum	Maximum
Cytosol		
NAD ⁺	520 [14]	730 [15]
NADH	18 [14]	55 [14]
NADP ⁺	140 [14]	145 [14]
NADPH	140 [14]	180 [14]
NADH:NAD ⁺	0.031 [14]	0.12 [13]
NADPH:NADP ⁺	1.0 [14]	1.8 [16]
Chloroplasts		
NAD ⁺	190 [15]	920 [15]
NADH	unknown	unknown
NADP ⁺	510 [15]	590 [15]
NADPH	120 [15]	290 [15]
NADH:NAD ⁺	0.24 [13]	0.4 [16]
NADPH:NADP ⁺	0.23 [15]	1.13 [13]
Mitochondria		
NAD ⁺	1410 [14]	1550 [14]
NADH	75 [14]	455 [14]
NADP ⁺	75 [14]	265 [14]
NADPH	45 [14]	235 [14]
NADH:NAD ⁺	0.07 [16]	2.6 [13]
NADPH:NADP ⁺	0.17 [14]	3.13 [14]

Table 2. Fluorescent biosensors for NAD(P)(H) including those already expressed in plants, available sensors not yet expressed in plants, and desirable sensors not yet developed

Sensor	Metabolite	K _d or midpoint	Dynamic range	Compartments	pH sensitive	Notes	Refs.
<i>In planta</i>							
SoNar	NADH:NAD ⁺	K _d NADH 0.2 μM K _{ratio} 0.036	15	plast, cyt,	Yes	True ratio sensor as signal is dependent on both NADH and NAD ⁺ .	[18,52]
iNap 1	NADPH	0.29 μM	9	plast, cyt, perox	Yes	Higher affinity sensor suitable for plant cytosol.	[18,62]
iNap 4	NADPH	30 μM	5	plast, cyt, perox	Yes	Lower affinity sensor suitable for plastids.	[18,62]
iNapC	N/A	N/A	N/A	plast, cyt, perox	Yes	Control sensor for pH correction of iNap and SoNar.	[18,62]
Peredox-mCherry	NADH:NAD ⁺	K _d NADH 1.2 μM K _{ratio} 0.0024	2.2	cyt	No	An NADH sensor compensated by NAD ⁺ concentration. Total pool or NAD ⁺ concentration must be considered.	[17,51]
Peredox-mCherry-DS	NADH:NAD ⁺	K _d NADH 31.4 μM K _{ratio} 0.0628	2.8	cyt	No	Lower affinity Peredox variant also with faster on/off binding kinetics.	[11]
<i>Available - Not yet in planta</i>							
Frex	NADH	3.7 μM (pH 7.4) 11 μM (pH 8.0)	9		Yes	FLIM cannot avoid pH sensitive signal.	[67]
LigA-cpVenus	NAD ⁺	65 μM	2		Yes	pH can be corrected by normalising to cpVenus control.	[68]
Apollo-NADP ⁺	NADP ⁺	0.1-20 μM	1.2		No	Fluorescence anisotropy based measurement.	[69]
NADPsor	NADP ⁺	2 mM	1.4		No	FRET based sensor.	[70]
<i>Desirable new sensors</i>							
	NADPH:NADP ⁺	K _{ratio} ~1.5		plast, cyt, perox, mit	No	Ligand binding sensor similar to Peredox or SoNar.	
	E _{NADP}	-350 to -450 mv		plast, cyt, perox, mit	No	Fuse NADP-dependent disulfide reductase to roGFP?	
	E _{NAD}	-250 to -350 mv		plast, cyt, perox, mit	No	Fuse NAD-dependent disulfide reductase to roGFP?	

Abbreviations: Plast, plastids; Cyt, cytosol; Perox, Peroxisomes; Mit, mitochondria.

Text Boxes

Box 1. The principle of fluorescent biosensors

(i) Biosensors are made up of a ligand binding protein (BP) and fluorescent protein (FP)(Figure I). (ii) Conformational change upon ligand binding causes a change in fluorescent properties. Two fluorescent signals are required for a ratiometric biosensor which allows internal normalisation for any changes in biosensor protein expression. (iii) In an ensemble of sensors, increasing ligand concentration increases the probability that the binding site on any one sensor will be occupied. The measured fluorescence intensity at λ_a and λ_b is proportional to the total number of sensors in the bound or unbound state. (iv) In this example fluorescence intensity at λ_a increases with increasing ligand concentration and λ_b decreases. (v) The binding affinity (K_d) of the sensor can be calculated *in vitro* by changing the ligand concentration and measuring the ratio of fluorescence intensity of λ_a/λ_b . (vi) Sensors can be calibrated *in vivo* by saturating the sensor to find R_{max} and desaturating the sensor to find R_{min} in the system being used. Note that R_{max} and R_{min} will vary depending on the instrument settings and fluorescence excitation power used and should therefore be measured at the same time as biological samples. Assuming the ligand concentration *in vivo* is much larger than the sensor concentration, and K_d is identical *in vivo* and *in vitro*, the ligand concentration can be calculated using Equation 1. R is the measured ratio of λ_a/λ_b , $I_{max \lambda_b}/I_{min \lambda_b}$ is the dynamic range of the fluorescence intensity in the second wavelength (λ_b) and n is the Hill coefficient.

$$\text{Equation 1. } [Ligand] = K_d \cdot \left(\frac{R - R_{min}}{R_{max} - R} \cdot \frac{I_{max \lambda_b}}{I_{min \lambda_b}} \right)^{\frac{1}{n}}$$

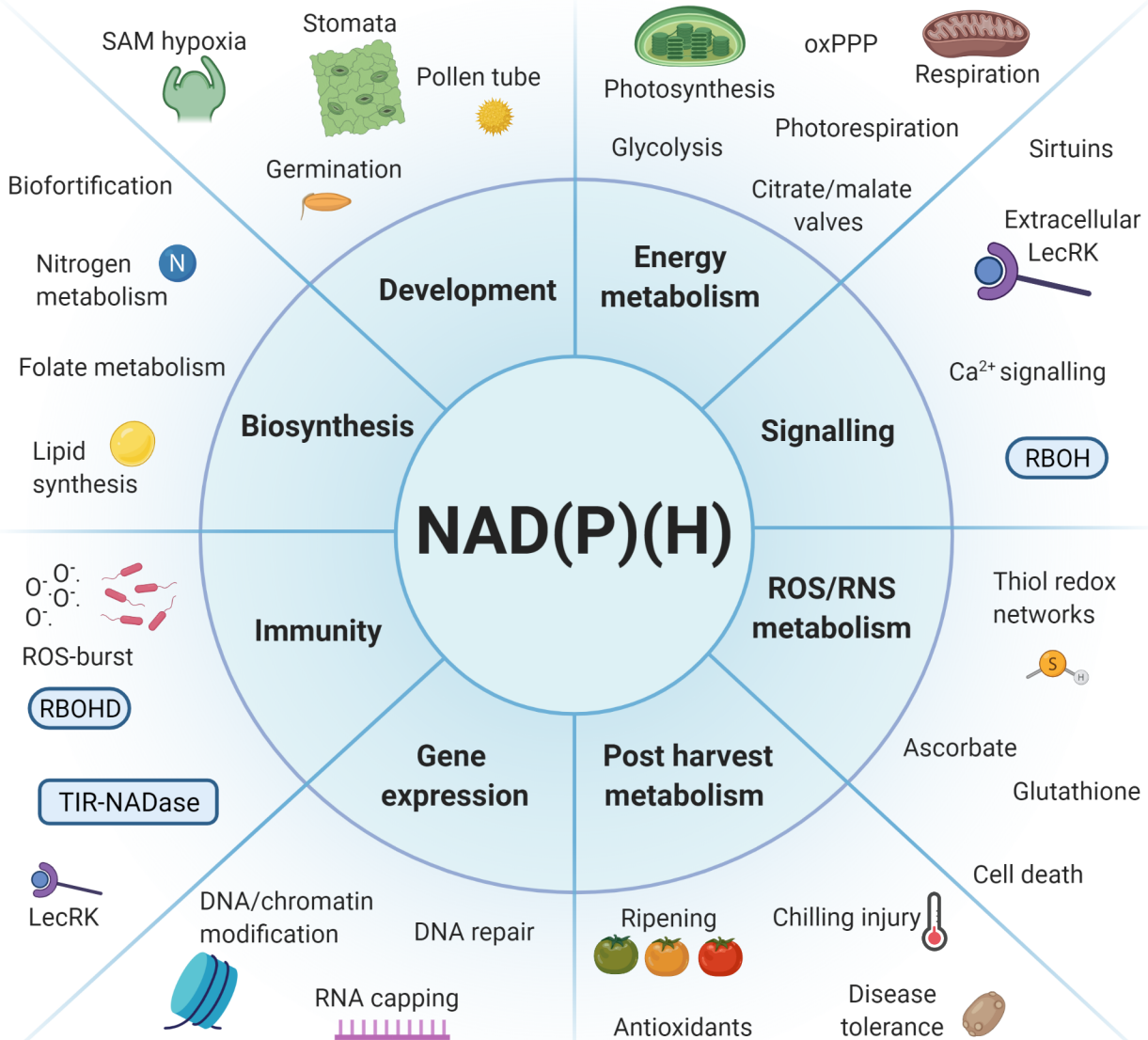
Glossary

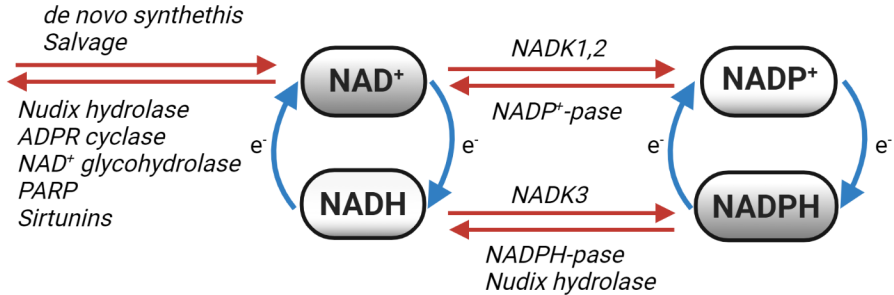
Circularly permuted fluorescent protein: The native N and C termini are fused through a linker, and new termini are created at the side of the barrel near the chromophore allowing close coupling of the chromophore with the ligand binding protein. There are many possible circularly permuted variants of a fluorescent protein depending on the linker and location of new N- and C-termini.

Dynamic range: The maximum fluorescence signal of the biosensor divided by the basal fluorescence signal.

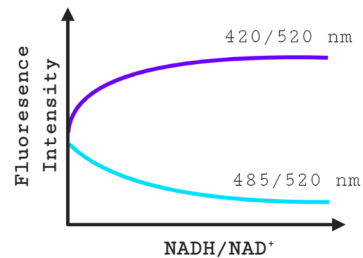
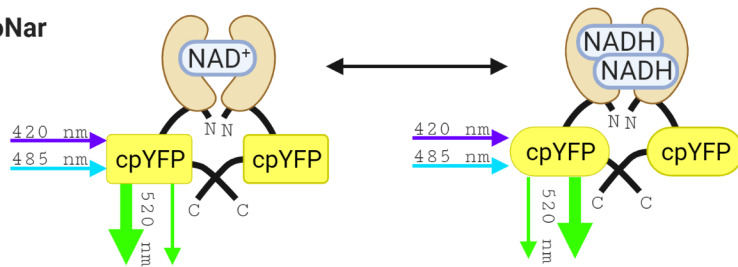
Operational range: The range of ligand concentrations which cause a change in fluorescence signal until a plateau is reached. Quantification becomes increasingly difficult as the signal plateaus due to the increased sensitivity of estimated ligand concentration to slight variation in signal intensity, and therefore a range between 5%-95% of the maximum and minimum signal is often used.

Sensor midpoint: The concentration of a single ligand or the ratio of competing ligands that produces half the maximal sensor response. Equivalent to the dissociation constant K_d or K_{ratio} .

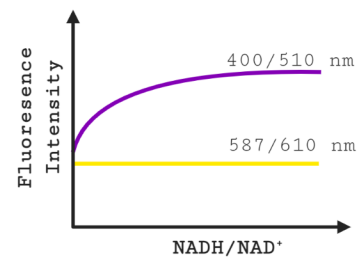
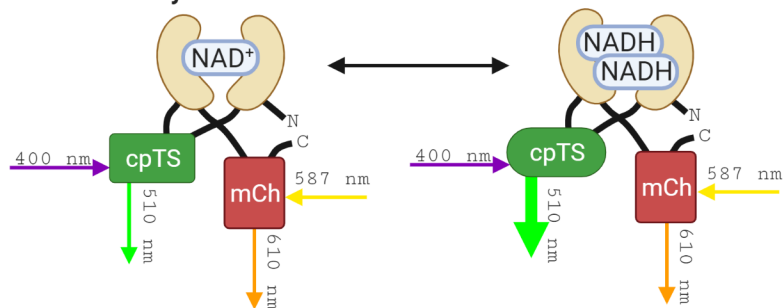




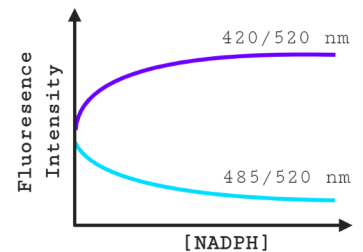
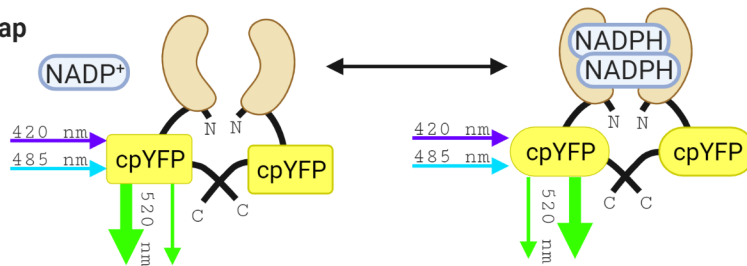
(A) SoNar

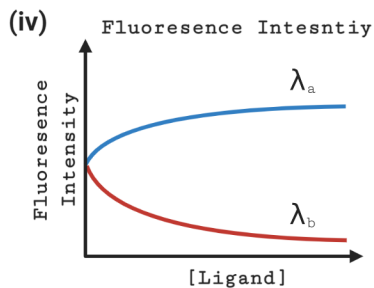
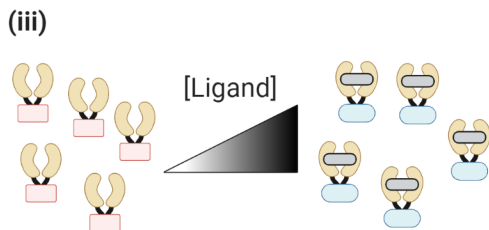
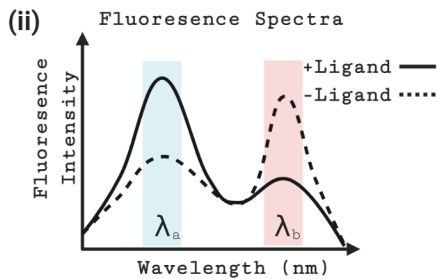
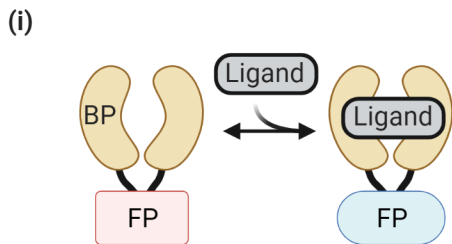


(B) Peredox-mCherry

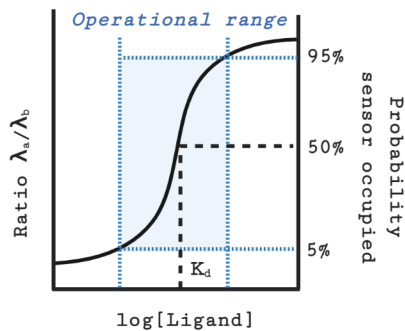


(C) iNap





(v) *In vitro* binding affinity



(vi) *In vivo* calibration

